communications biology

A Nature Portfolio journal

Article

https://doi.org/10.1038/s42003-025-08041-8

Phylogenetic and ecological drivers of the avian lung mycobiome and its potentially pathogenic component

Paris S. Salazar-Hamm[1,8] ✉, Chauncey R. Gadek[1,2,3,8] ✉, Michael A. Mann[1], Madeline Steinberg[1], Kyana N. Montoya[1,2], Mahgol Behnia[1], Ethan F. Gyllenhaal[1,2,4], Serina S. Brady[1,2,5], Oona M. Takano[1,2], Jessie L. Williamson[1,2,6,7], Christopher C. Witt[1,2] & Donald O. Natvig[1]

Vertebrate lungs contain diverse microbial communities, but little is known about the drivers of community composition or consequences for health. Microbiome assembly by processes such as dispersal, coevolution, and host-switching can be probed with comparative surveys; however, few studies exist for lung microbiomes, particularly for the fungal component, the mycobiome. Distinguishing among fungal taxa that are generalist or specialist symbionts, potential pathogens, or incidentally inhaled spores is urgent because of potential for emerging diseases. Here, we characterize the avian lung mycobiome and test the relative influences of environment, phylogeny, and functional traits. We used metabarcoding and culturing from 195 lung samples representing 32 bird species across 20 families. We identified 526 fungal taxa as estimated by distinct sequence types (zOTUs) including many opportunistic pathogens. These were predominantly from the phylum Ascomycota (79%) followed by Basidiomycota (16%) and Mucoromycota (5%). Yeast and yeast-like taxa (*Malassezia*, *Filobasidium*, *Saccharomyces*, *Meyerozyma*, and *Aureobasidium*) and filamentous fungi (*Cladosporium*, *Alternaria*, *Neurospora*, *Fusarium*, and *Aspergillus*) were abundant. Lung mycobiomes were strongly shaped by environmental exposure, and further modulated by host identity, traits, and phylogenetic affinities. Our results implicate migratory bird species as potential vectors for long-distance dispersal of opportunistically pathogenic fungi.

Vertebrate lung microbiomes and their fungal constituents (mycobiome) are emerging frontiers for ecology and public health. The emergence of antifungal-resistant pathogens[1–3] and climate-driven shifts affecting host reservoirs[4] underpin the urgency to describe the lung mycobiomes of diverse animal species. An essential task in understanding the public health implications of animal lung mycobiomes is parsing fungal taxa incidentally inhaled from exposure to airborne propagules[5] from taxa that colonize lung tissues and/or act as opportunistic pathogens; this has been challenging to assess due to the paucity of data on lung-fungal microbe associations[6]. One common approach to assess the relative contributions of incidental and specialized fungi to the lung mycobiome is to compare fungal taxa common in environmental samples (soil and air, for example) with taxa frequently encountered in lung mycobiome studies[7–9]. However, the lack of data on how fungal and host geographic distributions align complicates the identification of host-specialized taxa. A formerly prevailing view in fungal biogeography—that most fungi are not subject to the same dispersal barriers and biogeographic processes as plants and animal taxa—is now recognized as an oversimplification[10,11]. Although some fungal taxa have cosmopolitan ranges, many others conform to biogeographic barriers[12], which can result in false inference of host-specialization

Lungs, like other organs, have imposing immune defenses that act as a selective filter on microbial symbionts. The pulmonary mucosal immune response quickly clears most inhaled fungi; however, colonization can occur when innate immune defenses are diminished[13] or evaded by coevolved

[1]Department of Biology, University of New Mexico, Albuquerque, NM, USA. [2]Museum of Southwestern Biology, University of New Mexico, Albuquerque, NM, USA. [3]Environmental Stewardship, Los Alamos National Laboratory, Los Alamos, NM, USA. [4]Department of Biological Sciences, Texas Tech University, Lubbock, TX, USA. [5]Section of Birds, Carnegie Museum of Natural History, Pittsburgh, PA, USA. [6]Cornell Lab of Ornithology, Cornell University, Ithaca, NY, USA. [7]Department of Ecology and Evolutionary Biology, Cornell University, Ithaca, NY, USA. [8]These authors contributed equally: Paris S. Salazar-Hamm, Chauncey R. Gadek.
✉e-mail: psh102@unm.edu; cgadek@unm.edu

taxa[14]. Among many animals, apparent fungal associations and limited evidence for severe disease suggest deep shared evolutionary histories between lung fungi and their hosts[15]. Signs of coevolution, or phylosymbiosis, can elucidate the relative contributions of transient versus host-adapted taxa to the microbiome[16,17]. A few members of the microbiome have the capability to transcend host barriers and transmit from vertebrate animals to humans (zoonoses)[18]. Notably, rodents and bats have received attention because these spillover events have had devastating consequences for humans (e.g., coronaviruses[19], hantaviruses[20], and filoviruses[21]). However, a recent study of host-virus relationships found that host diversity explained the frequency of zoonoses that threaten humans more strongly than ecological or immunological traits[22]. Thus, expanding research to include a diverse array of vertebrate hosts is important to identify those likely to cause spillover events.

Among vertebrates, migratory birds require special consideration as a group with unique spillover potential because they are exposed to fungi in both feeding and nesting areas and at varying altitudes of flight[23,24]. Previous work on fungal opportunistic pathogens have highlighted several taxa linked to birds. For example, aspergillosis, caused by globally distributed species of *Aspergillus*, is perhaps the most widely recognized fungal infection (mycosis) of birds[25,26]. Documented on all continents except Antarctica[27], *Aspergillus* spp. (mainly *A. fumigatus*) typically cause disease when dosage thresholds are surpassed or exposed individuals are immunocompromised[28]. Species of *Candida* have also been identified as common commensals of birds and occasionally implicated in bird mycoses[29,30]. Bird guano is considered a natural reservoir for *Cryptococcus neoformans* causing cryptococcosis, which can have severe presentations in humans such as fungal meningitis[31–33]. Several other species of *Cryptococcus* (e.g., *C. gattii*, *C. uniguttulatus*, and *C. laurentii*) have been isolated from multiple bird species and are occasionally implicated in human and bird mycoses[34–36]. Considering that concern about emerging fungal pathogens is increasing, identifying potential pathways of exposure is paramount.

Of the over 11,000 bird species currently recognized[37], ~20% are migratory; yet, there has been no comprehensive survey of the avian lung mycobiome or its potential to be a reservoir for undescribed, host-generalist and specialist pathogens. Many migratory birds travel thousands of kilometers during migration, suggesting that they may be important vectors capable of transporting and dispersing fungi over long distances, even spanning hemispheres[38]. Specifically, birds have been insinuated in the transport of *Candida auris*, a multidrug-resistant pathogenic yeast[39]. The connection between life history traits like migration and the transport of fungal pathogens highlights the importance of characterizing avian mycobiomes and testing potential drivers of mycobiome diversity and composition. It is critical to account for host phylogeny because the susceptibility of birds to diverse pathogens has been shown to be phylogenetically conserved[40]. Microbial diversity may additionally be driven, in part, by host traits[41–44] like body size, tissue pH, and diet, as well as aspects of the environment such as seasonality and precipitation[45]. Long-distance migration and flight might obscure ecologically or phylogenetically driven variation in the mycobiomes of host species, which are exposed to locally distinct fungal communities at different times of the year[46,47]. Yet, the presence of fungal lineages specialized on particular host clades could remain discernible despite the homogenization resulting from host dispersal.

To the best of our knowledge, we report the first comprehensive characterization of the avian lung mycobiome, derived from migratory and resident birds from the southwestern USA. Using both fungal metabarcoding and culture data, we compared lung mycobiomes among 32 bird species, and identified host-associated fungal species and potential pathogens. We then tested fungal-host associations at multiple host-phylogenetic levels, from avian subspecies to order. To evaluate the relative contributions of environment versus hosts, we tested for host phylogenetic signal of lung fungal alpha diversity, compared fungal community differences among hosts with disparate breeding ranges, migration strategies, foraging modes, and sampling years. We additionally modeled fungal community differences as a function of geographic distance, dispersal-related traits, and host phylogeny and evaluated co-occurrence patterns among fungal lung taxa. Our results revealed moderately diverse lung-fungal communities that were subtly structured by aspects of host life history and phylogeny. Many of the identified fungal lineages are potential opportunistic pathogens that were non-randomly associated with migratory sandhill cranes. Our multi-pronged characterization of avian lung mycobiome reveals factors driving mycobiome community assembly at evolutionary timescales and the potential role of birds as agents of fungal dispersal.

Results

Sample acquisition

Of the 195 avian lung tissues, 120 were from greater sandhill cranes (*A.c. tabida*) and 26 were from lesser sandhill cranes (*A.c. canadensis*) from Valencia and Socorro counties, New Mexico, collected between November and December 2019 and in January 2020. The remaining 49 bird lungs were obtained from specimens salvaged across ten New Mexican counties (Bernalillo, Chaves, Curry, Eddy, Los Alamos, Rio Arriba, Sandoval, Santa Fe, San Juan, and Taos) between 2006 and 2018. In total, we examined the mycobiome of 195 avian lung samples representing 33 taxa across 20 families within 12 orders.

Lung mycobiome community analysis

After removing samples that did not pass DNA quality and quantity standards, we performed Illumina ITS2 metabarcoding on 183 avian lung tissues. After filtering non-fungal reads, we removed 16 samples with less than 2000 reads each. The final avian lung mycobiome community dataset was composed of 167 samples: 100 greater sandhill cranes, 22 lesser sandhill cranes, and 45 salvaged birds (Supplementary Data 1). Our metabarcoding efforts produced a total of 6,656,903 fungal reads clustered into 526 zOTUs. On average, sequencing yielded 39,862 reads per sample although this varied substantially ($\sigma = 35{,}984$). The greatest number of fungal reads were captured from a common loon (*Gavia immer*; MSB:Bird:60464; reads=240,528), a barn owl (*Tyto alba*; MSB:Bird:60463; reads=145,669), and a marsh wren (*Cistothorus palustris*; MSB:Bird:60445; reads=141,996).

Rarefaction curves indicated substantial coverage of fungal diversity (Supplementary Fig. 1). Taxonomic assignment with UNITE and GenBank (BLASTn) databases were largely concordant. Taxa were predominantly within the phylum Ascomycota (79.4%) followed by Basidiomycota (15.9%) and Mucoromycota (4.6%). One zOTU fell within Chytridiomycota and one zOTU could not be identified to phylum using either database. The most abundant and frequent zOTUs were from the Malasseziomycetes (*Malassezia*) and Tremellomycetes (*Filobasidium*) within Basidiomycota, and the Dothideomycetes (*Cladosporium*, *Alternaria*, and *Aureobasidium*), Eurotiomycetes (*Thermomyces* and *Aspergillus*), Sordariomycetes (*Neurospora* and *Fusarium*), and Saccharomycetes (*Meyerozyma*, *Saccharomyces*, and *Clavispora*) within Ascomycota (Fig. 1). Twelve zOTUs could not be identified at the class level. We identified ten Malasseziomycetes, which included the two most prevalent zOTUs in the community dataset: zOTU2 detected in all 167 samples and zOTU21 found in 158 (94.6% of the samples). Additional diversity of basidiomycetous yeasts fell within the Tremellomycetes ($n = 36$ zOTUs) and included 24 *Cryptococcus*-like yeasts (e.g., species of *Naganishia*, *Vishniacozyma*, and *Filobasidium*) (Supplementary Fig. 2). The most frequent and abundant was *Filobasidium* (*Cryptococcus*) *magnum* (zOTU20) detected in 112 samples (67.1%). Among the Ascomycota the greatest representation was from the Eurotiomycetes (118 zOTUs, 28.2%). Of note, 56 of these zOTUs were classified within the family Aspergillaceae of which 6 (zOTU19, zOTU467, zOTU849, zOTU990, zOTU1294, and zOTU3349), were classified as *Aspergillus fumigatus*, the primary causative agent of aspergillosis (Supplementary Fig. 3). Due to the use of zOTUs it is possible that some taxa, like *A. fumigatus*, may be over split into several zOTUs because of intra-species or intra-individual variation. The dominant taxon from this group, zOTU19, was detected in 96 samples (57.5%) and represented greater than a third of the sequences from two greater sandhill cranes (*Antigone canadensis tabida*, MSB:Bird:56461, 90% and MSB:Bird:56426, 36%) and a common loon

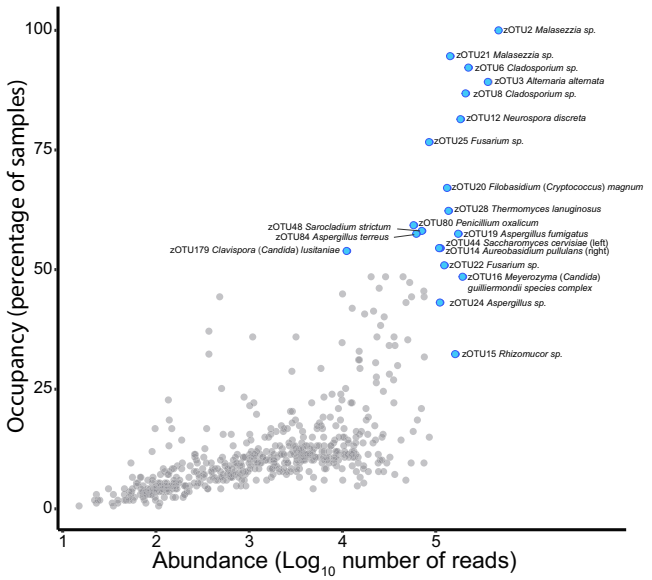

Fig. 1 | Relationship between occupancy and abundance. Occupancy is represented by percent of lung samples and abundance by $\log_{10}$ number of reads for 526 zOTUs. Blue dots and labeling indicate those zOTUs with occupancy in >50% of samples and/or with a read abundance of >5 $\log_{10}$.

(*Gavia immer*, MSB:Bird:60464, 36%), although it was otherwise generally in low abundance (0–5% of reads). Dothideomycetes were the second most prevalent ascomycete (103 zOTUs, 24.6%) and included two species of *Cladosporium* (zOTU6 in 92.2% and zOTU8 in 86.8% of samples), *Alternaria alternata* (zOTU3 in 89.2% of samples), and to a lesser extent *Aureobasidium pullulans* (zOTU 14 in 54.5% of samples; Fig. 1). We also noted a great diversity (57 zOTUs) within the ascomycetous yeast order Saccharomycetales. This order contained several etiological agents of human candidemia including *Clavispora* (*Candida*) *lusitaniae* (zOTU179 in 53.9% of samples), *Meyerozyma* (*Candida*) *guilliermondii* complex (zOTU16 in 52.1% of samples), *Candida tropicalis* (zOTU233 in 39.5% of samples), *Pichia kudriavzevii* (*Candida krusei*, zOTU576 in 10.2% of samples), and *Candida parapsilosis* (zOTU47 in 6.8% of samples; Fig. 1, Supplementary Fig. 4).

We cultured 300 fungal isolates from 107 avian lungs. At least one fungus was isolated from 55% of the lungs plated. The majority of pure cultures ($n = 274$, 91.3%) were isolated from sandhill cranes. Cultures were sorted by morphotype followed by preliminary identification by sequencing the ribosomal ITS region. A total of 171 sequences from fungal cultures were obtained representing 48 operational taxonomic units (OTUs) when clustered at 97% similarity (Table 1, Supplementary Data 2). Most of the cultures belonged to Ascomycota ($n = 239$, 79.7%) followed by Mucoromycota ($n = 53$, 17.7%) and Basidiomycota ($n = 8$, 2.7%). The most abundant and diverse class was the Eurotiomycetes ($n = 121$, 18 OTUs). Within the Eurotiomycetes (order Eurotiales) there was great diversity within the genera *Aspergillus* (7 OTUs; Supplementary Fig. 3), *Penicillium* (5 OTUs), and *Talaromyces* (4 OTUs). *Talaromyces purpureogenus* was the second most commonly cultured taxon ($n = 45$, 15.0%). The second most abundant class was Dothidiomycetes ($n = 64$) of which half the cultures were from a single species of *Cladosporium*. The third most commonly cultured taxon was within the Sordariomycetes ($n = 50$), which is a member of the *Fusarium fujikuroi* species complex (FFSC, $n = 23$). The Mucoromycota fungi all fell within Mucoromycetes ($n = 53$) and were identified within the genera *Lichtheimia, Mucor*, and *Rhizopus*. The most frequently isolated fungus of the entire culture collection was *Rhizopus arrhizus* ($n = 46$, 15.3%) obtained from 45 individual cranes. Many cultures shared high sequence similarity with the uncultured community dataset. For example, we isolated six *Filobasidium* (*Cryptococcus*) *magnum* cultures related to zOTU20 (Supplementary Fig. 2), one *Papiliotrema* (*Cryptococcus*) *flavescens* culture related to zOTU637 (Supplementary Fig. 2), and four *Meyerozyma guilliermondii* complex cultures related to zOTU16 (Supplementary Fig. 4). In one instance, a cultured fungus putatively identified as *Malbranchea albolutea* was unique to sequences in the community dataset, but it was similar to OTU84 (OK078109) detected in mammal lungs (Supplementary Fig. 5).

Alpha and beta diversity

Mean zOTU richness for the full dataset rarefied to the minimum sampling depth of 2056 reads was 41.8 ± 19.7 among all lung samples (range = 9–125; Supplementary Figs. 6a and 7). Although most fungi appeared to be host-generalist, several fungal orders were detected only in sandhill crane samples: Botryosphaeriales (9 zOTUs, reads = 2704), Coniochaetales (zOTU1303, reads = 9), Filobasidiales (zOTU499, reads = 309), Hymenochaetales (3 zOTUs, reads = 1392), Leucosporidiales (zOTU78, reads = 1472), Lichenostigamtales (3 zOTUs, reads = 2512), Melanosporales (zOTU1013, reads = 139), Onygenales (7 OTUs, reads = 815), Polyporales (zOTU485, reads = 1854), Russalales (zOTU208, reads = 2007), and Tritirachiales (zOTU1795, reads = 7). Although ~67% of sampled birds in our dataset were cranes, the orders Atractiellales (zOTU1329, reads = 5), Boletales (zOTU2438, reads = 1), Entylomatales (zOTU1341, reads = 6), and Erysiphales (zOTU228, reads = 1141), represented by singleton zOTUs, were found only in non-crane samples. Among all lung samples, the mean Shannon diversity was 1.50 ± 0.75 (range = 0.20–3.56; Supplementary Fig. 6b), the Chao1 index was 55.39 ± 29.21 (range = 9–175.6; Supplementary Fig. 6c), and the mean inverse Simpson's index was 3.79 ± 2.98 (range = 1.06–24.5; Supplementary Fig. 6d). We found no phylogenetic signal in any of the lung fungal community alpha diversity estimates for both the full rarefied dataset or the rarefied animal-symbiont subset of zOTUs (Supplementary Table 1).

Fungal beta diversity differed among avian orders ($n = 167$, $R = 0.168$, $P = 0.002$), although these differences appeared to be driven by the strong sampling of cranes (without cranes: $n = 45$, $R = -0.030$, $P = 0.638$). Phylogenetic and Bray-Curtis dissimilarity showed little correspondence but some conspecifics (*Antigone*) and closely related taxa (*Astur cooperii* and *Accipiter striatus*) fell adjacent to one another in Bray-Curtis matrices suggesting shallow intra-specific host specificity (Fig. 2). Fungal diversity differed among avian host life history traits, including migration strategy ($n = 167$, $R = 0.175$, $P = 0.002$; Supplementary Fig. 8a) and foraging guild ($n = 167$, $R = 0.113$, $P = 0.019$; Supplementary Fig. 8b). After removing cranes, where the lesser and greater subspecies differ substantially in migration distance (Fig. 3a, b), foraging guild remained a significant driver of fungal diversity ($n = 45$, $R = 0.239$, $P = 0.0004$), and migration became marginally significant ($n = 45$, DF = 2, $F = 1.343$, $R^2 = 0.060$, $P = 0.0416$). We found no differences between subspecies ($n = 122$, DF = 1, $F = 1.231$, $R^2 = 0.010$, $P = 0.132$) when analyzing data for only cranes. Hybridization occurs between *A. c. tabida* and *A. c. canadensis* resulting in intermediate forms, and the inclusion of intermediates could obscure differences in fungal diversity. However, we excluded suspected intermediates from the dataset and therefore anticipate that few unidentified intermediates remained in our analyses. When testing just the subset of zOTUs that included only animal symbionts as identified with FUNGuild, we observed a signal of avian order ($n = 167$, $R = 0.111$, $P = 0.021$) and a marginal signal of foraging guild ($n = 195$, $R = 0.091$, $P = 0.046$); however, in this comparison, migratory strategy ($n = 167$, $R = 0.066$, $P = 0.142$) was not significant. Beta diversity among sampling years was highly significant for all bird species ($n = 167$, $R = 0.175$, $P = 9.999e^{-05}$; Supplementary Fig. 8c) and when subsetting by only sandhill cranes ($n = 122$, $R = 0.106$, $P = 9.999e^{-05}$), but not when subsetting for only non-crane bird species ($n = 45$, $R = -0.70$, $P = 0.905$). The signal held for the animal symbiont subset of the mycobiome ($n = 167$, $R = 0.124$, $P = 9.999e^{-05}$), but not when subsetting by only non-crane host species ($n = 45$, $R = 0.046$, $P = 0.268$).

A Mantel test showed a non-significant correlation between geographic distance and fungal community dissimilarity ($n = 167$, $r = 0.0336$, $P = 0.14$); however, positive spatial autocorrelation was seen from 0 km to

Table 1 | Fungal taxa from 300 avian lung cultures

Phylum	Class	Order	Genus	Species	UNITE species hypothesis	Number of cultures	Number of birds
Ascomycota	Dothideomycetes	Pleosporales	*Alternaria*	*A. alternata*	SH0856386.10FU	14	13 (7.9%)
				A. malorum	SH0856971.10FU	1	1 (0.6%)
			Ascochyta	*A. medicaginicola*	SH0862152.10FU	1	1 (0.6%)
			Curvularia	*Curvularia* sp.	SH0856683.10FU	2	2 (1.2%)
			Didymella	*Didymella* sp.	SH0862152.10FU	5	5 (3.0%)
			Neocamarosporium	*N. betae*	SH0960158.10FU	1	1 (0.6%)
			Tamaricicola	*Tamaricicola* sp.	SH0856892.10FU	2	2 (1.2%)
		Cladosporiales	*Cladosporium*	*Cladosporium* sp.	SH0962330.10FU	32	27 (16.5%)
		Dothideales	*Aureobasidium*	*Aureobasidium* sp.	SH0925964.10FU	3	3 (1.8%)
		Incertae sedis	*Coniosporium*	*Coniosporium* sp.	SH0932560.10FU	1	1 (0.6%)
		unclassified	unclassified	unclassified	SH1005923.10FU	1	1 (0.6%)
	Eurotiomycetes	Chaetothyriales	*Rhinocladiella*	*Rhinocladiella* sp.	SH0986920.10FU	3	2 (1.2%)
		Eurotiales	*Aspergillus*	*A. fumigatus*	SH0940075.10FU	16	11 (6.7%)
				A. niger	SH0731269.10FU	12	8 (4.9%)
				A. neoniveus	SH0984584.10FU	1	1 (0.6%)
				A. terreus	SH0984584.10FU	4	2 (1.2%)
				Aspergillus sp. 1	SH0940487.10FU	3	3 (1.8%)
				Aspergillus sp. 2	SH0940476.10FU	1	1 (0.6%)
				Aspergillus sp. 3	SH0888267.10FU	1	1 (0.6%)
			Penicillium	*P. decumbens*	SH0767693.10FU	1	1 (0.6%)
				Penicillium sp. 1	SH0939544.10FU	8	8 (4.9%)
				Penicillium sp. 2	SH0939872.10FU	13	12 (7.3%)
				Penicillium sp. 3	SH0767731.10FU	1	1 (0.6%)
				Penicillium sp. 4	SH0940404.10FU	1	1 (0.6%)
			Talaromyces	*T. piceae*	SH0973364.10FU	1	1 (0.6%)
				T. minioluteus	SH0901331.10FU	1	1 (0.6%)
				T. pinophilus	SH0901369.10FU	8	5 (3.0%)
				T. purpureogenus	SH0901369.10FU	45	39 (23.8%)
		Onygenales	*Malbranchea*	*M. albolutea*	SH0875561.10FU	1	1 (0.6%)
	Saccharomycetes	Saccharomycetales	*Meyerozyma*	*M. guilliermondii*	SH0887053.10FU	4	4 (2.4%)
	Sordariomycetes	Hypocreales	*Beauveria*	*B. bassiana*	SH0740100.10FU	5	4 (2.4%)
			Fusarium	FFSC sp. 1	SH0731064.10FU	23	18 (11.0%)
				FFSC sp. 2	SH0731064.10FU	14	12 (7.3%)
				FIESC	SH0731269.10FU	2	2 (1.2%)
		Microascales	*Microascus*	*M. cirrosus*	SH0934581.10FU	1	1 (0.6%)
		Myrmecridiales	*Myrmecridium*	*M. schulzeri*	SH0982314.10FU	1	1 (0.6%)
		Sordariales	*Chaetomium*	*C. globosum*	SH0978756.10FU	1	1 (0.6%)
			Neurospora	*N. discreta*	SH0904979.10FU	2	2 (1.2%)
			Parachaetomium	*Parachaetomium* sp.	SH0978522.10FU	1	1 (0.6%)
Basidiomycota	Microbotryomycetes	Sporidiobolales	*Rhodotorula*	*Rhodotorula* sp.	SH0877557.10FU	1	1 (0.6%)
	Tremellomycetes	Filobasidiales	*Filobasidium*	*F. magnum*	SH0857509.10FU	6	6 (3.7%)
		Tremellales	*Papiliotrema*	*P. flavescens*	SH1016500.10FU	1	1 (0.6%)
Mucoromycota	Mucoromycetes	Mucorales	*Lichtheimia*	*L. corymbifera*	SH0855590.10FU	1	1 (0.6%)
				L. ramosa	SH0884010.10FU	2	2 (1.2%)
			Mucor	*M. irregularis*	SH1020240.10FU	1	1 (0.6%)
				M. circinelloides	SH0747765.10FU	3	3 (1.8%)
			Rhizopus	*R. arrhizus*	SH0980336.10FU	46	45 (27.4%)

Contigs are clustered at 97% similarity.

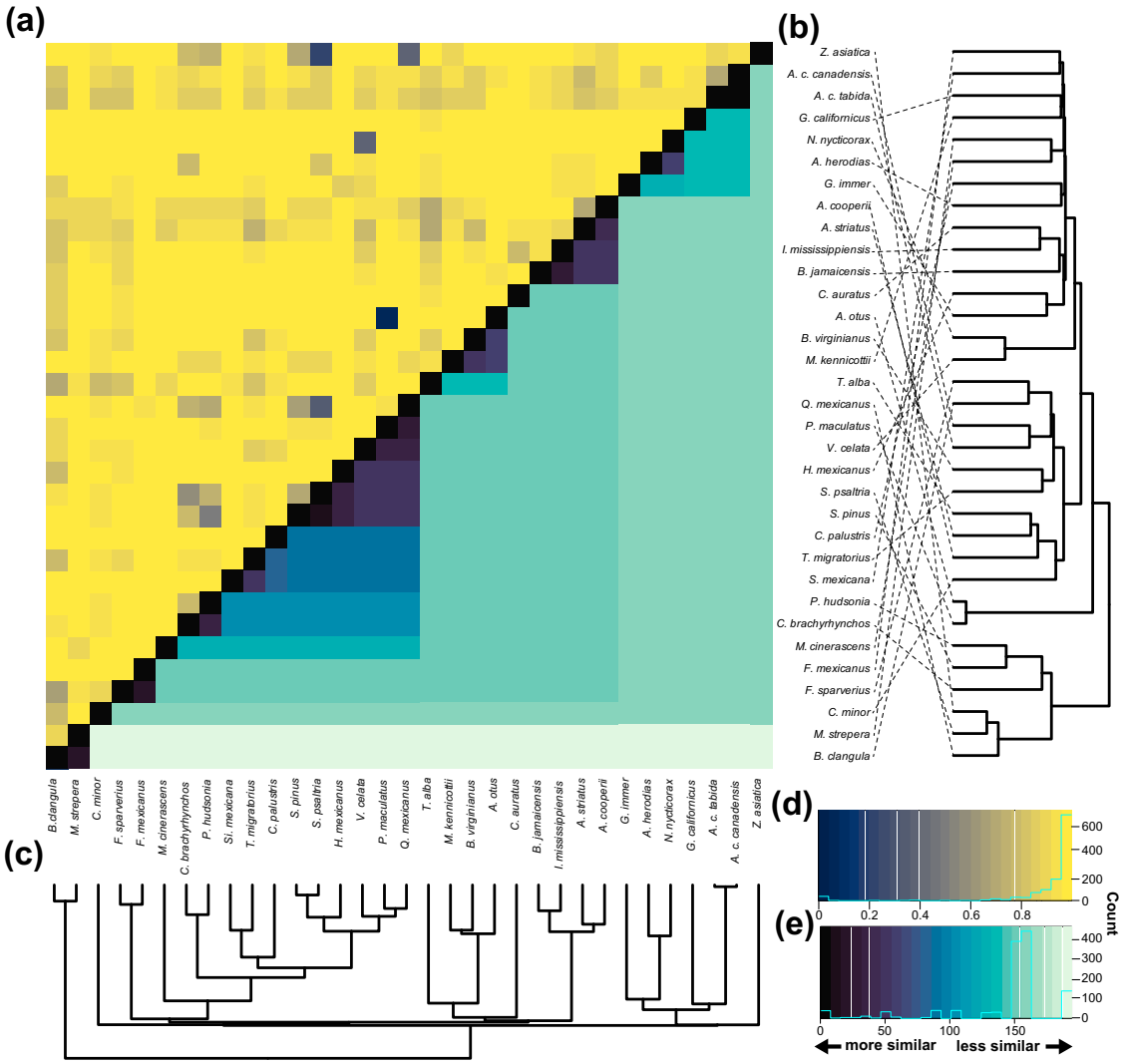

Fig. 2 | Little correspondence between fungal beta diversity and host phylogenetic diversity. a The heatmap indicates fungal community differences as the average of Bray-Curtis distances of 1000 community matrices, repeatedly rarefied to the minimum sampling depth (2056 reads) in the upper left and phylogenetic distance calculated from branch lengths of the maximum clade credibility tree generated from a sample of 100 topologies downloaded from birdtree.org in the lower right. Color scales for Bray-Curtis and phylogenetic distances are indicated by the *x*-axes of (**d**, **e**). **b** A tanglegram shows correspondence (dashed lines) between the phylogenetic tree and dendrogram generated from Bray Curtis distances. **c** A maximum clade credibility tree pruned to match host taxa in our dataset. **d** A histogram showing distribution of Bray-Curtis distances. **e** A histogram showing the distribution of phylogenetic distance.

58 km ($P = 0.034$), indicating that samples collected closer together tended to have more similar fungal communities (Supplementary Fig. 9). A Mantel test on a subset of the data where cranes were removed also showed no significant correlation between geographic distance and fungal community dissimilarity ($n = 45$, $r = -3.35e^{4}$, $P = 0.459$).

FUNGuild assigned coarse functional guilds at the class or genus level for 462 zOTUs (87.8%). Avian lungs contained substantial numbers of putative animal symbionts. Every sample contained at least one fungal zOTU designated as an animal symbiont. The average abundance of fungal animal symbionts per avian sample was 44.1%; however, this varied greatly between samples ($\sigma = 33.9\%$, range = 1.47–67.7%). Although not statistically significant (*t*-test, DF = 10,079, $t = -0.072$, $P = 0.943$), the average abundance of animal symbionts among sandhill cranes was higher in greater sandhill cranes (45.2%) than lesser sandhill cranes (42.7%; Fig. 3c). Within both lineages of sandhill crane, we further assessed the prevalence of a subset of fungal animal symbionts with representatives implicated as pathogens. Both subspecies had a roughly equivalent mean prevalence of zOTUs from Onygenales (lesser: 12.7 ± 3.04%, greater: 10.6 ± 3.71%), *Cryptococcus*-like yeasts (lesser: 21.3 ± 19.9%, greater: 24.3 ± 18.3%), Saccharomycetales (lesser: 18.2 ± 14.6%, greater: 16.6 ± 14.7%), and Aspergillaceae (lesser: 20.2 ± 15.9%, greater: 24.3 ± 18.3%; Fig. 3d).

Fungal co-occurrence

We found evidence for microbial interactions among taxa of the core avian mycobiome. Co-occurrence associations of the core mycobiome families ranged from −0.302 to 0.330 (Spearman rank-abundance). There were more positive associations (71.4%) than negative associations (28.6%) among the core mycobiome members (Supplementary Fig. 10, Supplementary Table 2). The strongest positive correlation (Spearman rank correlation coefficient; ρ) was found between Filobasidiaceae, a family of *Cryptococcus*-like yeasts, and Cladosporiaceae ($n = 167$, $\rho = 0.330$, $P = 1.33e^{-05}$; Supplementary Table 2). The greatest negative correlation was between Aspergillaceae and Coniosporiaceae ($n = 167$, $\rho = -0.302$, $P = 7.47e^{-05}$; Supplementary Table 2). Co-occurrence associations calculated as Spearman rank-abundance of the animal-symbiont subset of the mycobiomes ranged from −0.188 to 0.254. There were again more positive associations (57.1%) relative to negative associations (42.9%) among the animal-symbiont mycobiome members (Supplementary Fig. 11,

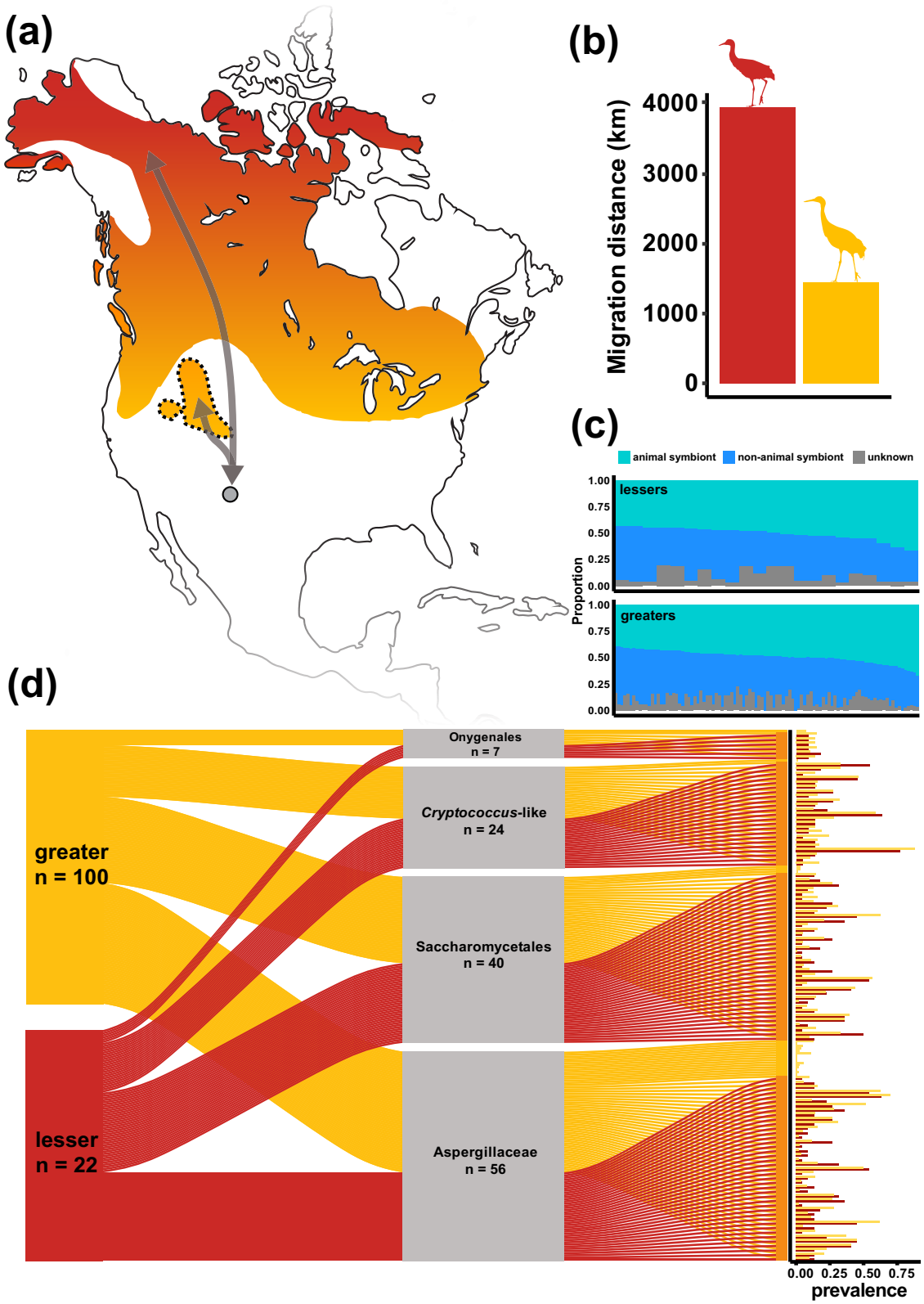

Supplementary Table 3). The strongest positive correlation was between Aspergillaceae and Trichocomaceae ($n = 167$, $\rho = 0.254$, $P = 9.18e^{-04}$; Supplementary Table 3). The strongest negative association was between Filobasidiaceae and Trichocomaceae ($n = 167$, $\rho = -0.188$, $P = 0.015$; Supplementary Table 3).

Generalized dissimilarity modeling

Aspects of host biology and evolutionary history best explained the dissimilarity among fungal communities. The GDMs explained a modest amount of the dissimilarity among the fungal communities ($n = 33$, mean deviance explained 9.02% ± 0.25). The predictors with the highest summed

Fig. 3 | Sandhill crane subspecies differences in animal symbiont components of the lung mycobiome. Comparison of geographic range, migratory distances, and potential animal symbiont and opportunistic pathogen composition of mycobiome between lesser and greater sandhill cranes. **a** Range map of approximate breeding locations and shared wintering sampling location of lesser (red) and greater (yellow) sandhill cranes. The Rocky Mountain population of greater sandhill cranes (source population for this study) is emphasized with a dashed outline. Migration stopover location in New Mexico where sampling occurred is indicated with a gray circle. Gray arrows emphasize relative differences in migratory distance. **b** Approximate mean migratory distances of lesser and greater sandhill cranes. **c** Relative abundance of pooled putative fungal animal symbionts assigned with FUNGuild[59] for greater (top) and lesser (bottom) sandhill cranes. Each bar along the x-axis represents a single sample. **d** Relative compositions of potential opportunistic pathogens in lung mycobiome of each subspecies. Widths of connecting ribbons between crane subspecies and fungal clade indicate the relative proportion of pathogen clade in total candidate pathogen zOTU pool of each crane subspecies. Ribbons connect fungal clades to zOTUs. The zOTUs are colored red if recovered from lesser sandhill cranes or yellow for greater sandhill cranes. Barplot on the right shows the percent prevalence of each zOTU by crane subspecies.

I-spline coefficients were hand-wing index (0.574 ± 0.498), followed by host phylogenetic distance (0.228 ± 0.332), and migratory distance (0.143 ± 0.203); Supplementary Fig. 12, Supplementary Table 4). The predictors with the highest importance were hand-wing index (38.8 ± 1.59% Dev−variable *i*−Dev), followed by migration distance (23.4 ± 1.23% Dev −variable *i*−Dev), and host phylogenetic distance (10.3 ± 0.643 Dev −variable *i*−Dev; Supplementary Fig. 12, Supplementary Table 4).

Discussion

This study provides an initial characterization of the lung mycobiome of wild birds. The average of 41.8 ± 19.7 zOTU richness recovered from bird lungs (Supplementary Figs. 6a and 7) was comparable to the fungal richness found in a recent survey of the rodent lung mycobiome[8]. However, estimates of lung zOTU richness were lower than for previously characterized mycobiomes from the avian gut[48,49] and arid soil[50]—though certain individuals, like a barn owl (MSB:Bird:60463) and an orange-crowned warbler (MSB:Bird:60434), showed comparably high zOTU richness. After accounting for fungal abundance and taxonomic evenness using the Shannon diversity index, there was still substantial variation among bird species in our dataset (0.20–3.56; Supplementary Fig. 6b). Differences in microbiome diversity among organ systems are well documented for bacterial communities[51–53] and may reflect local, organ-specific adaptation of microbes.

Fungal richness also varied substantially among individuals within avian host species (Supplementary Fig. 7). For example, barn owl ($n = 4$; MSB:Bird:60459, MSB:Bird:60448, MSB:Bird:60458, MSB:Bird:60463) mycobiome richness ranged from 9 to 125 zOTUs. Similar ranges of intraspecies fungal richness were recovered from mammalian lungs[8]. High variation in gut mycobiome diversity among individuals within host taxa has been previously documented in wild birds[48] and is likely driven, in part, by the spatial and temporal heterogeneity of fungal cells in the environment.

We found high levels of lung mycobiome differences among bird taxa ($n = 33$, $\bar{x}$ Bray-Curtis dissimilarity = 0.94 ± 0.01; Fig. 2). This pattern could be produced by stochastic assembly due to incidental inhalation from a heterogeneous microbial environment, or it could reflect host specialization or differential filtering of fungal taxa due to host ecology or immunology. Many mycobiomes of closely related hosts had higher Bray-Curtis dissimilarity than those between more distantly related host taxa (Fig. 2). Only the similar mycobiomes within sandhill cranes and between closely related hawk species provided evidence of host phylogenetic effects on community assembly. Otherwise, the tendency for large differences in microbiome composition between bird hosts at various phylogenetic distances emphasizes the roles of environmental heterogeneity and incidentally inhaled fungi as drivers of variation in the core lung mycobiome of birds.

Although our dataset suggests that the lung mycobiome of birds is assembled largely by heterogeneous environmental exposure, we found evidence of phylosymbiosis at shallow host phylogenetic levels (Fig. 2, Supplementary Fig. 12, Supplementary Table 4). Host specialization was evident within a widespread and morphologically variable species (the sandhill crane, *Antigone canadensis*) and between the *Accipiter* and *Astur* genera of hawks (Fig. 2). Although these associations could reflect coevolved symbioses at shallow phylogenetic levels, we cannot rule out that they could be the result of shared ecologies among closely related taxa.

Dietary effects on the differentiation of gut microbial communities have been commonly reported in the literature[42,48], but whether and to what degree dietary and foraging differences shape the lung mycobiome has been less clear. We found that carnivorous taxa, like falcons, showed some of the lowest Shannon diversity values (Supplementary Fig. 6b). Tests of beta diversity confirmed significant fungal community differences among dietary guilds (Supplementary Fig. 8b). Lung mycobiome composition and dietary habits may be linked in instances where species with specialized foraging strategies and substrates inhale different local fungal cells. For example, species probing in mud and foraging in agricultural fields are exposed to more saprotrophic and soil-associated fungal taxa through feeding than aerial hunters or "salliers" that rarely encounter soil fungal communities. Likewise, nesting and roosting behavior may play a role in differentiating lung fungal communities by exposing species to various fungal microbes associated with nesting materials and general nest locations. Future comparative work could evaluate lung mycobiome differences among cavity, cup, and ground-nesting species.

Bird species that breed or winter in geographically isolated regions are likely exposed to distinct fungal communities, potentially influencing their lung mycobiomes. However, our results offered limited and inconsistent support for this hypothesis. We detected significant differences in fungal communities among bird species with different migratory strategies (Supplementary Fig. 8a), even after excluding sandhill cranes from the dataset. Migration distance and hand-wing index emerged as the strongest predictors of fungal community dissimilarity in GDMs, though the models themselves explained little overall variation (Supplementary Fig. 12). A Mantel test found an insignificant correlation between geographic distance and fungal community dissimilarity; however, samples that were within 58 km were more similar (Supplementary Fig. 9). A separate analysis of fungal communities between sandhill crane subspecies, which differ greatly in migratory distance and hand-wing index, revealed no significant differences (Fig. 3). These discrepancies may be the result of reduced statistical power, as our analysis relied on summary estimates for crane samples, masking substantial overlap in these covariates. Despite these limitations, the absence of fungal community differences in cranes—despite their wide breeding ranges and distinct migratory behaviors—and the weak explanatory power of GDMs suggest that lung mycobiome assembly in our sampled bird community is largely passive, driven by the spatial and temporal variation of fungal microbes.

Skeen et al. found significant year effects on bacterial beta diversity among four species of *Catharus* thrush[47]. Indeed, we found a strong effect of sampling year on fungal beta diversity, highlighting how temporal change in exposure to fungal cells may be an important driver of fungal lung diversity (Supplementary Fig. 8c) even among animal-symbiont taxa. All crane individuals in our dataset were collected in the same region during the nonbreeding season in late fall and winter, when they shared the same riparian and agricultural habitats. Lung fungal communities that may be differentiated on the breeding grounds could equilibrate, and therefore become less distinguishable on shared wintering areas. Seasonal equilibration could occur rapidly after arrival in shared wintering areas; a study on broiler chickens showed that it took only 3 days for their initial mycobiota to be replaced with environmental fungi from dietary sources[49]. Another study found rapid temporal shifts in the bacterial gut microbiome of blackpoll

warblers during migration which was attributed to changes in host physiological and energetic demands[54]. Further work comparing samples between species collected at their breeding and wintering sites, across different life stages, and at various time points during the annual cycle could offer more insights into how shared and isolated ranges impact lung microbiomes.

One of the goals of the current study was to evaluate the frequency with which fungi that are known to be opportunistic pathogens occur in the lungs of healthy wild birds. Substantial attention has been given to the potential for birds to serve as vectors for disease[55–57]. Although direct transmission of bacterial, fungal, and viral diseases from wild birds to humans may be rare[58], the role of birds in pathogen transmission is also important for both domestic and wild animals. This is particularly relevant for opportunistic fungal pathogens because many of these organisms typically act as saprotrophs in non-host environments. A few studies have addressed the potential for migratory birds to harbor and disperse pathogenic and non-pathogenic fungi[59,60]. The present study found a wide variety of known opportunistic lineages alongside many putative animal symbionts.

In a previous study of the lung mycobiome, Salazar-Hamm et al. identified sequences from multiple opportunistic fungal pathogens (e.g., *Aspergillus fumigatus*, as well as species of *Candida, Pneumocystis*, *Blastomyces*, and *Coccidioides*) that were common in small mammals of New Mexico, Arizona, and California[8]. Bird lungs differed from mammalian lungs in that *Pneumocystis* and *Coccidioides* were absent, a result that was anticipated given that species of *Pneumocystis* are considered to be obligate lung pathogens of only mammals, and birds do not seem to be common reservoir hosts for *Coccidioides* (whether because of differences in host behavior or immunity). However, as in mammalian lungs, bird lungs possessed multiple other opportunistic fungal pathogens including *Aspergillus fumigatus, Blastomyces parvus*, *Clavispora* (*Candida*) *lusitaniae*, members of the *Meyerozyma* (*Candida*) *guilliermondii* complex, *Filobasidium* (*Cryptococcus*) *magnum*, and members of Mucorales (Fig. 1, Table 1). This commonality may largely reflect the commensal nature of many fungi generally considered to be pathogens[6,61].

Not only did our extensive host sampling using frozen tissues from the MSB facilitate comparisons among the lung fungal communities of diverse bird species, but it also allowed us to make detailed intra-specific comparisons between two subspecies of sandhill crane. The smaller-sized lesser sandhill crane can migrate over 3000 km to breed at high latitudes in northern Canada, Alaska (USA), and Eastern Russia, whereas the overwintering greater sandhill cranes are thought to migrate less than 1500 km between New Mexico and the northern Rocky Mountains[62] (Fig. 3b). On their New Mexico wintering grounds, state-managed hunting and foraging at agricultural sites place these large-bodied migratory birds in close contact with human populations. Accordingly, migration could relocate pathogens with subsequent opportunities for transmission to other hosts. The number of fungal zOTUs representing potential animal symbionts, including fungal pathogens, was highly variable among individual cranes (Fig. 3c). These zOTUs represent several fungal groups that are important to human and animal health (Onygenales, Saccharomycetales, Aspergillacaeae, and *Cryptococcus*-like yeasts) (Fig. 3d).

Dimorphic fungi within Onygenales can evade immune responses of healthy hosts and cause disease. The mammalian lung mycobiome exhibits significant diversity and abundance of members within the order Onygenales (e.g., *Blastomyces parvus* and *Emmonsia*-like species)[8,63]; however, they appear to be less common in birds, and in the community dataset, they were only recovered from cranes (Supplementary Fig. 5). *Blastomyces parvus* (zOTU392, zOTU464, zOTU616, zOTU706, zOTU1008, and zOTU1670) and *Spiromastigoides asexualis* (zOTU1347), detected in the community dataset, as well as the *Malbranchea albolutea* culture isolated from an American robin (*Turdus migratorus*, MSB:Bird:60476) may be examples of animal commensals that can but on rare occasions cause disease[6,64,65]. Coccidioidomycosis, caused by the Onygenalean fungi *Coccidioides immitis* and *Coccidioides posadasii*, is endemic to the southwestern U.S. including New Mexico[66]. Although this disease is largely confined to mammals, there has been a few rare reports in other animal hosts including birds[67,68]. While *Coccidioides* was absent from our avian dataset, it was reported in 12% of mammals from this same region[8].

We sought to evaluate whether migratory birds act as reservoirs for high-priority *Candida* species[69], as hypothesized for *Candida auris*[39]. Although *C. auris* was not detected here, we did capture many other opportunistic pathogens within Saccharomycetales (e.g., species of *Candida*, *Meyerozyma*, *Pichia*, *Clavispora, Spathaspora*, and *Debaryomyces*)[70] (Supplementary Fig. 4). The closest relative to *C. auris* identified in our dataset was *Clavispora* (*Candida*) *lusitaniae*, an infrequent cause of human candidemia (~1% of cases), but a species for which several emerging antifungal-resistant strains have been documented[71]. *Pichia kudriavzevii* (*Candida krusei*), another infrequent etiological agent of human candidemia (~3% of cases), is notable because, similar to *C. auris* strains, it is intrinsically resistant to fluconazole[72]. *Candida parapsilosis* and *Candida tropicalis*, the third (~12% of cases) and fourth (~7% of cases) most common agents causing candidemia worldwide[73], were also detected in our avian lungs.

In addition to *A. fumigatus*, other species of *Aspergillus* (e.g., *A. terreus*, *A. flavus*, and *A. niger*) that can cause allergic asthma to invasive pulmonary aspergillosis[25] in humans and animals were detected in avian fungal communities (Supplementary Fig. 3). Because pathogenic or lethal doses must be considerably higher for immunocompetent individuals (~10^6 spores per individual[74–76]), the low abundance of these sequences across the majority of bird samples suggests these are present as a result of transient inhalation of spores from the environment and/or are low-load commensals rather than agents of chronic or acute infections[9,77]. Our study and others[8,9,78] have reported high loads of *Aspergillus* in the lungs of healthy humans and animals, which may also suggest that other factors such as host susceptibility or strain virulence may be important to the outcome of infection.

Species within the genus *Cryptococcus* have been frequently isolated from bird cloacae and feces[29,79,80], suggesting birds may be important reservoirs and dispersers of opportunistic yeast pathogens. Our study identified a wide diversity of Tremellomycetes yeasts (e.g., species of *Naganishia*, *Vishniacozyma*, and *Filobasidium*) in bird lungs, many previously identified as *Cryptococcus* species prior to reclassification[81,82] (Supplementary Fig. 2). While none of these taxa are now assigned to *Cryptococcus*, and those detected are rarely pathogenic[83,84], evidence of direct transmission of closely related yeasts[31] suggests that birds in close contact with human populations have spillover potential, albeit low. Our findings further indicate a high diversity of low-virulence reclassified *Cryptococcus* yeasts (class Tremellomycetes) that are associated with the avian gut[85] and lung mycobiome.

Climate change is expected to alter host-fungal pathogen dynamics in multiple ways. Casadevall et al. used phylogenetic analyses of thermal tolerance to argue that *C. auris* evolved as a competitive animal symbiont as a result of selection imposed by a warming climate[39]. The geographic ranges of several fungal pathogens are shifting or expected to shift in response to climate change[4,86]. As the distributions of pathogenic fungi expand, novel overlaps between fungal and avian ranges are expected to occur, thereby increasing opportunities for migratory birds to transport fungi over long distances.

The lung mycobiomes of wild birds are diverse, with substantial variation among individuals and species. Diversity observed in this study was comparable to that found in small mammals previously sampled in the same region. Host phylogenetic effects on lung-fungal community assembly were evident at shallow phylogenetic scales in both cranes and hawks. Within cranes, the two subspecies sampled at shared wintering grounds exhibited a largely shared lung mycobiome. We found no direct effects of higher-level host phylogeny on fungal communities. These patterns generally support environmental exposure as the main driver of fungal lung communities, with substantial stochastic variation. We identified numerous putative animal symbionts and potential pathogens among the migratory bird lungs we surveyed. Although the emerging (*Candida auris*) and endemic (*Coccidioides* spp.) fungal pathogens were absent among the bird lungs that we surveyed, we did detect close fungal relatives (e.g., *Blastomyces parvus*,

Spiromastigoides asexualis, *Malbranchea albolutea*, and other species of *Candida*) that should be monitored in the context of potential pathogenesis. Our study suggests that host-pathogen dynamics among bird species, and the potential for long-distance pathogen transport, are tied to the fungi of local environments to which birds are exposed. Predicted changes in host and fungal species distributions in response to climate warming are expected to result in novel host lung-fungi combinations and altered host-fungi dynamics.

Methods

Sample acquisition

We sampled lung tissues ($n = 195$) from migratory and resident bird species salvaged throughout New Mexico, USA representing 32 species within 20 families (Supplementary Data 1). The majority were hunter-donated tissues from two subspecies of sandhill cranes (*Antigone canadensis*, $n = 146$). The remaining ($n = 49$) were salvaged after death by private individuals and wildlife rescue organizations and subsequently donated to the Museum of Southwestern Biology (MSB). Lung tissues were frozen on dry ice and stored in −80 °C freezers before being archived in vapor phase nitrogen freezers (−196 °C) in the MSB Division of Genomic Resources at the University of New Mexico (UNM). We identified cranes to subspecies (*A.c. canadensis* and *A.c. tabida*) in the field using several diagnostic morphological parameters including mass, wing chord length, culmen length, and tarsus length. All birds were sexed internally by inspecting gonads during dissection and aged by the presence and size of the bursa of Fabricious (present in young birds); cranes were additionally aged by plumage and iris coloration. Precise GPS coordinates of sampling locations were not available for many salvaged avian samples. To estimate sample location, we calculated the latitude and longitude centroids of the county where each bird was recovered using the R package geosphere[87]. We additionally recorded the date of salvage to assess temporal variation in fungal communities.

Ecological and behavioral variables of avian hosts

Using published data (AVONET[88] database and reported estimates[62]) and expert knowledge, for each species in the dataset we assigned feeding guild, range size in km^2, migration distance in km, and mean hand-wing index (a measure of avian flight ability)[89] to each species in the dataset. We included the recorded mass in grams of individual birds; when mass was not recorded, we included the mean species mass as reported in the AVONET dataset. A map of the ranges for sandhill crane subspecies was created using the R packages rnaturalearth[90] v.1.0.1 and naturalearthdata[91] v.1.0.0.

Illumina ITS2 metabarcoding and processing

We lyophilized approximately 25 mg of lung tissue for 24 h, and then performed a CTAB DNA extraction[8] followed by an AMPure bead (Agencourt Bioscience Corporation, Beverly, MA, USA) purification. The ITS2 rRNA region was amplified with the ITS3F and ITS4R primers[92,93] in a 30-cycle PCR reaction using the HotStarTaq Plus Master Mix Kit (Qiagen Inc, Cambridge, MA, USA) under the following conditions: 95 °C for 5 min, followed by 30 cycles of 95 °C for 30 s, 53 °C for 40 s and 72 °C for 1 min, after which a final elongation step at 72 °C for 10 min was performed. PCR products were checked on a 2% agarose gel. Based on DNA quality and quantity, 183 samples were multiplexed and pooled in equal proportions based on molecular weight and DNA concentrations. Pooled products were purified using Ampure XP beads (Beckman Coulter Inc, Brea, CA, USA) following manufacturer instructions and were used to create DNA libraries following the Illumina MiSeq DNA library preparation protocol for paired-end reads. Samples were sequenced by MR DNA on an Illumina MiSeq Shallowater, Texas (http://www.mrdnalab.com). The raw reads were submitted to the NCBI Short Read Archive (SRA) under BioProject PRJNA1136563.

We used USEARCH[94] v.11.0.667 to merge paired-end reads, remove adapters and primers, and perform quality filtering using a maximum expected error threshold of 1.0. With UNOISE3[95], we performed error correction (denoised) on unique sequences and clustered them into zero-radius operational taxonomic units (zOTUs), employed to distinguish between species and strains that would otherwise be grouped together. Initial taxonomic assignment was performed with the SINTAX[96] algorithm against the UNITE v.10 all eukaryotes database[97] and confirmed with NCBI BLASTn (Supplementary Data 3). We removed all non-fungal (Metazoa and Viridiplantae) sequences. We evaluated sufficient sequencing depth using the *rarecurve* function in vegan[98] v.2.6-4.

Assignment of trophic mode

We used FUNGuild[99] v.1.1 to assign trophic modes (i.e., pathotroph, saprotroph, or symbiotroph) and functional guilds to fungal zOTUs. Animal-fungal symbionts from each sample were pooled by determining the percent of reads in each sample that belonged to zOTUs whose guild assignments included animal pathogen, animal parasite, and animal symbiotroph.

Identification of core mycobiome

The core mycobiome refers to the common set of fungal zOTUs in a host taxon. To identify the core lung mycobiome of the migratory birds in our dataset, we first transformed the full dataset to proportional abundances and filtered the zOTUs, keeping only those zOTUs that were detected in >50% of bird samples and with >0.01% relative abundance. We then ran the function *core* from the package microbiome[100], to obtain a subset of core taxa and used it for downstream co-occurrence analyses.

Alpha and beta diversity

We rarefied the full data set using the *rarefy_even_depth* function in phyloseq[101] v.1.48.0 using the sample with the fewest reads as the target sample depth. Rarefaction to a minimum sampling depth of 2056 reads removed 18 zOTUs leaving 508 zOTUs for downstream diversity analyses. We also rarefied subsets of putative animal symbionts and non-symbionts as assigned by FUNGuild to minimum sampling depths of 58 and 39 respectively. Using the full rarefied community data, we calculated zOTU richness, Chao1 index, Shannon diversity index, and inverse Simpson index using the function *estimate_richness* from the phyloseq[101] package. We used non-metric multidimensional scaling (NMDS) to explore drivers of diversity and visualize groupings of fungal lung communities into host phylogenetic, demographic, and ecological categories. To visually compare lung mycobiome beta diversity and host phylogenetic diversity we first merged fungal reads by summing within avian host taxa, then repeatedly ($n = 1000$) rarefied to the minimum sampling depth of 2056 reads, calculated the Bray-Curtis dissimilarity index between samples, and averaged the resulting matrices. We then used the averaged matrix to generate a heatmap and corresponding dendrogram using the function *heatmap2* from the package gplots[102] v.3.1.3.1. We generated a phylogenetic distance matrix from the maximum clade credibility (MCC) tree (see phylogenetic analyses below) with the *cophentic_phylo* function from the R package ape[103] v.5.8. To visualize phylogenetic patterns among lung fungal communities, we arranged the beta diversity matrix according to the order of the phylogenetic distance matrix. We plotted the phylogenetic distance matrix below the beta diversity matrix and created a tangle-gram to indicate discordance between the phylogenetic tree and the Bray-Curtis dissimilarities. To test for differences in bird fungal assemblages among multiple life history traits and phylogenetic scales, we used Bray–Curtis and PERMANOVA (permutational multivariate analysis of variance) models (Bray-Curtis ~ group, 10,000 permutations) using the *adonis2* function in vegan[98] v. 2.8-6. If there were differences in multivariate dispersion assessed with the *betadispr* function from vegan[98], an ANOSIM (analysis of similarities) test was used in lieu of a PERMANOVA. We repeated PERMANOVA and ANOSIM tests of community dissimilarity with a subset of host taxa including only cranes, another with only non-crane bird species, and fungal taxa containing known animal symbionts and opportunistic pathogens. We investigated the correlation between geographic distance and fungal community similarity using a Mantel correlogram and Mantel test in vegan[98]. Because similarity is

expected to decrease with geographical distance, we plotted distance decay by computing Bray-Curtis between each pair of samples along a spatial gradient.

Co-occurrence analyses

To evaluate microbial associations within the avian mycobiome, we ran co-occurrence analyses on the core fungal zOTUs and the core taxa from the rarefied subset of animal symbionts. We calculated Spearman rank abundance correlations and tested for significant correlations using the *co_occurrence* function from the phylosmith[104] package v.1.0.6. We used the *co_occurrence_network* function from phylosmith[104] to plot co-occurrence patterns.

Generalized dissimilarity modeling

We used generalized dissimilarity modeling (GDM) in the R package gdm[105] v.1.5.0-9.1 to evaluate fungal-host phylogenetic associations and test the effects of geographic and morphological correlates of dispersal and migration on host fungal community dissimilarity. GDM predicts changes in beta diversity over space, time, and environmental gradients and allows the inclusion of several types of distance matrices as response and predictor variables (e.g., Jaccard, phylogenetic distance). GDMs use linear combinations of I-splines to model changes in predictors across ecological distance with the relative heights of the I-splines[105,106]. Using rarefied abundance-weighted fungal zOTU tables, we calculated Bray-Curtis dissimilarity matrices as response variables in our GDMs. To address uneven sampling, we ran 1000 GDMs on datasets of abundances summed within avian host species repeatedly rarefied to the minimum sampling depth of 2056 reads. To examine the effect of host phylogenetic distance on fungal community dissimilarity, we additionally generated a phylogenetic distance matrix from the MCC tree using the *cophentic_phylo* function from the R package ape[101]. We tested the effects of five predictor variables: host mass, species hand-wing index, range size (km^2), migratory distance (km), and host phylogenetic distance on Bray-Curtis matrices of fungal community dissimilarity. We scaled or log_{10} transformed each predictor. We extracted and plotted all I-splines regardless of their significance from each of the 1000 fitted models. We used the *gdm.varImp* function from the gdm[105] package to evaluate model fit and variable importance among all 1000 models.

Cultured lung fungi

We plated a portion (25–50 mg) of each lung sample on yeast glucose media (1% yeast extract, 2% glucose, 1.5% agar) with the addition of antibiotics tetracycline (10 mg/L) and chloramphenicol (50 mg/L) to reduce bacterial growth. Each plate received 3–5 fragments (~0.25 cm each) of tissue from a single lung. Plates were incubated at room temperature for 2 days to 3 months depending on fungal growth rate. Individual yeast colonies or hyphal tips were transferred to fresh media to obtain single-isolate cultures. We sorted isolates based on morphology and chose representative isolates for molecular barcoding of the nuclear ribosomal internal transcribed spacer (ITS) region. We extracted DNA following a standard CTAB procedure with an isoamyl alcohol-chloroform extraction. Subsequently, we amplified the DNA using polymerase chain reaction (PCR) with ITS1-F and ITS4[92,107]. The following PCR cycle was implemented: initial denaturation at 95 °C for 10 min, followed by 34 cycles of 95 °C for 15 s, annealing at 52 °C for 30 s, and extension at 72 °C for 1 min, with a final extension at 72 °C for 5 min. We confirmed products with gel electrophoresis and purified them with ExoSAP-IT (Affymetrix, Santa Clara, CA, USA) following manufacturer recommendations. The entire ITS region was targeted for Sanger sequencing using BigDye Terminator v3.1 (Applied Biosystems, Foster City, CA, USA), and the sequences were identified using BLAST[108]. If samples within one morphotype varied in taxonomic classification, we sequenced additional fungal cultures for more accurate identification. We identified *Fusarium* sequences to species complexes by employing FUSARIUM-ID[109] v.3.0. We deposited sequences in GenBank under accession numbers PP804255-PP804425 (Supplementary Data 2).

Phylogenetic analyses

We explored the diversity of amplicon sequences and cultured isolates for select fungal groups that have consequences for human and animal health using a phylogenetics approach with ribosomal ITS sequences. These included Aspergillacaeae, Onygenales, and Saccharomycetales fungi, as well as *Cryptococcus*-like yeasts (e.g., species of *Naganishia*, *Vishniacozyma*, and *Filobasidium*). Reference sequences from GenBank[110] as well as those from our previous study of the lung communities of small mammals in the southwestern U.S[8]. were included (Supplementary Data 4). We aligned sequences with mafft[111,112] v.7.487 using automatically determined settings and trimmed the resulting alignment with trimal[113] v.1.4.1 in *automated1* mode. The final alignments were 697 bases for Aspergillaceae, 263 bases for *Cryptococcus*-like yeasts, 540 bases for Onygenales, and 301 bases for Saccharomycetales, and they were deposited in Dryad (https://doi.org/10.5061/dryad.hqbzkh1t3). We inferred maximum likelihood trees with the best fitting model according to ModelFinder[114] in IQ-Tree[115] v.1.6.12 with 10,000 ultrafast bootstraps. The best fitting model was TIM2e+G4 for Aspergillaceae, TVMe+I+G4 for *Cryptococcus*-like yeasts, TNe+G4 for Onygenales, and HKY+F+I+G4 for Saccharomycetales. Phylogenies were rooted with standard outgroups explicitly *Aspergillus fumigatus* for Onygenales[116], *Coccidioides immitis* for Aspergillaceae[117], *Mycosarcoma* (*Ustilago*) *maydis* for *Cryptococcus*-like yeasts[82], and *Neurospora crassa* for Saccharomycetales[118]. The resulting trees were visualized in ggtree[119]. Nexus-formatted alignments and Newick trees were deposited in Dryad (https://doi.org/10.5061/dryad.hqbzkh1t3) and are available in Supplementary Data 5.

We tested the level of host phylogenetic signal in alpha diversity indices: zOTU richness, Shannon diversity, inverse Simpson, and Chao1. For each alpha diversity index, we calculated a mean value at the host taxon level from the full rarefied dataset as trait inputs for tests of phylogenetic signal. We downloaded a set of 10,000 phylogenetic trees from https://birdtree.org/ with the *Hackett backbone*[120,121] and generated a MCC tree using the function *maxCladeCred* from the R package phangorn[122] v.2.5.5. We then pruned the tree to the taxa in our dataset using the *keep.tip* function in ape[103]. We tested for phylogenetic signal using Moran's I, Abouheif's Cmean, and Pagel's Lamda tests using the R packages adephylo[123] v.1.1-13 and phytools[124] v.2.0. We evaluated adjusted *P* values against a 0.05 significance level from permutation tests ($n = 10{,}000$) to identify phylogenetic signal in each alpha diversity metric.

Statistics and reproducibility

To address the effects of uneven and limited sample sizes across avian species and ecological groups, we conducted separate analyses on subsets of host taxa. One analysis included only cranes, which comprised the majority of our samples, while another focused on non-crane bird species. See "Methods" section for details.

Statistical analyses were performed using phyloseq[101] v.1.48.0, vegan[98] v.2.8-6, phylosmith[104] v.1.0.6, gdm[105] v.1.5.0-9.1, and adephylo[123] v.1.1-13. Reported *P*-values include all significant digits, with a significance threshold of 0.05. Datasets and code, including the seeds used in our original analysis, are available as links in *Data availability* and *Code availability* statements.

Mycobiome sequence data were obtained from frozen lung tissues of preserved biological specimens from natural history collections. These specimens are linked to publicly available geographical data and a comprehensive set of host metadata, ensuring reproducibility and expandability of host-parasite research[125,126]. We provide museum records, as ARCTOS database links for all samples and GenBank accession numbers for our fungal sequence data. Datasets for both full and rarified fungal community analyses were deposited in Zenodo[127].

We characterized the avian lung mycobiome using a dual approach: fungal culturing and metabarcoding. This combination allowed us to capture a broader diversity of fungi while mitigating the biases inherent in each method.

Reporting summary

Further information on research design is available in the Nature Portfolio Reporting Summary linked to this article.

Data availability

All sequence data generated in this study is linked to host voucher specimens from the Museum of Southwestern Biology archived in the ARCTOS museum database (https://arctos.database.museum). Select host metadata is also available in Supplementary Data 1. Raw mycobiome sequences were deposited in GenBank Short Read Archives (BioProject PRJNA1136563). Taxonomic assignment of zOTUs from the UNITE v.10 database are available in Supplementary Data 3. Datasets for both full and rarified fungal community analyses were deposited in Zenodo (https://zenodo.org/records/15098514). Nexus-formatted alignments and Newick trees for the fungal phylogenetic analyses are available in Dryad (https://doi.org/10.5061/dryad.hqbzkh1t3) and Supplementary Data 5. The ribosomal ITS sequences generated from the fungal cultures were deposited in GenBank's nucleotide database under accessions: PP804255-PP804425 (Supplementary Data 2).

Code availability

Code and source data are on GitHub (https://github.com/cgadek/Bird_Mycobiome) and Zenodo (https://zenodo.org/records/15098514).

Received: 6 October 2024; Accepted: 4 April 2025;
Published online: 19 April 2025

References

1. Satoh, K. et al. *Candida auris* sp. nov., a novel ascomycetous yeast isolated from the external ear canal of an inpatient in a Japanese hospital. *Microbiol. Immunol.* **53**, 41–44 (2009).
2. Daneshnia, F. et al. Worldwide emergence of fluconazole-resistant *Candida parapsilosis*: current framework and future research roadmap. *Lancet Microbe* **4**, e470–e480 (2023).
3. Snelders, E. et al. Emergence of azole resistance in *Aspergillus fumigatus* and spread of a single resistance mechanism. *PLoS Med.* **5**, e219 (2008).
4. Salazar-Hamm, P. & Torres-Cruz, T. J. The impact of climate change on human fungal pathogen distribution and disease incidence. *Curr. Clin. Microbiol. Rep*. https://doi.org/10.1007/s40588-024-00224-x (2024).
5. Fröhlich-Nowoisky, J., Pickersgill, D. A., Després, V. R. & Pöschl, U. High diversity of fungi in air particulate matter. *Proc. Natl. Acad. Sci. USA* **106**, 12814–12819 (2009).
6. Hamm, P. S., Taylor, J. W., Cook, J. A. & Natvig, D. O. Decades-old studies of fungi associated with mammalian lungs and modern DNA sequencing approaches help define the nature of the lung mycobiome. *PLOS Pathog.* **16**, e1008684 (2020).
7. Kramer, R. et al. Cohort study of airway mycobiome in adult cystic fibrosis patients: differences in community structure between fungi and bacteria reveal predominance of transient fungal elements. *J. Clin. Microbiol.* **53**, 2900–2907 (2015).
8. Salazar-Hamm, P. S. et al. Breathing can be dangerous: opportunistic fungal pathogens and the diverse community of the small mammal lung mycobiome. *Front. Fungal Biol.* **3**, 996574 (2022).
9. Rubio-Portillo, E. et al. The domestic environment and the lung mycobiome. *Microorganisms* **8**, 1717 (2020).
10. Fröhlich-Nowoisky, J. et al. Biogeography in the air: fungal diversity over land and oceans. *Biogeosciences* **9**, 1125–1136 (2012).
11. Taylor, J. W., Turner, E., Townsend, J. P., Dettman, J. R. & Jacobson, D. Eukaryotic microbes, species recognition and the geographic limits of species: examples from the kingdom Fungi. *Philos. Trans. R. Soc. B Biol. Sci.* **361**, 1947–1963 (2006).
12. Sato, H., Tsujino, R., Kurita, K., Yokoyama, K. & Agata, K. Modelling the global distribution of fungal species: new insights into microbial cosmopolitanism. *Mol. Ecol.* **21**, 5599–5612 (2012).
13. Bartemes, K. R. & Kita, H. Innate and adaptive immune responses to fungi in the airway. *J. Allergy Clin. Immunol.* **142**, 353–363 (2018).
14. Medrano, F. J. et al. *Pneumocystis jirovecii* in general population. *Emerg. Infect. Dis.* **11**, 245–250 (2005).
15. Elliott, T. F. et al. A global review of the ecological significance of symbiotic associations between birds and fungi. *Fungal Divers.* **98**, 161–194 (2019).
16. Phillips, C. D. et al. Microbiome analysis among bats describes influences of host phylogeny, life history, physiology and geography. *Mol. Ecol.* **21**, 2617–2627 (2012).
17. Trevelline, B. K., Sosa, J., Hartup, B. K. & Kohl, K. D. A bird's-eye view of phylosymbiosis: weak signatures of phylosymbiosis among all 15 species of cranes. *Proc. R. Soc. B Biol. Sci.* **287**, 20192988 (2020).
18. Plowright, R. K. et al. Pathways to zoonotic spillover. *Nat. Rev. Microbiol.* **15**, 502–510 (2017).
19. Li, W. et al. Bats are natural reservoirs of SARS-like coronaviruses. *Science* **310**, 676–679 (2005).
20. Jonsson, C. B., Figueiredo, L. T. M. & Vapalahti, O. A global perspective on hantavirus ecology, epidemiology, and disease. *Clin. Microbiol. Rev.* **23**, 412–441 (2010).
21. Towner, J. S. et al. Marburg virus infection detected in a common African bat. *PLoS ONE* **2**, e764 (2007).
22. Mollentze, N. & Streicker, D. G. Viral zoonotic risk is homogenous among taxonomic orders of mammalian and avian reservoir hosts. *Proc. Natl. Acad. Sci. USA* **117**, 9423–9430 (2020).
23. Damialis, A. et al. Estimating the abundance of airborne pollen and fungal spores at variable elevations using an aircraft: how high can they fly? *Sci. Rep.* **7**, 44535 (2017).
24. Pace, L., Boccacci, L., Casilli, M. & Fattorini, S. Temporal variations in the diversity of airborne fungal spores in a Mediterranean high altitude site. *Atmos. Environ.* **210**, 166–170 (2019).
25. Seyedmousavi, S. et al. *Aspergillus* and aspergilloses in wild and domestic animals: a global health concern with parallels to human disease. *Med. Mycol.* **53**, 765–797 (2015).
26. Arné, P. et al. *Aspergillus fumigatus* in poultry. *Int. J. Microbiol.* **2011**, 1–14 (2011).
27. Converse, K. A. Aspergillosis. in *Infectious Diseases of Wild Birds* (eds. Thomas, N. J., Hunter, D. B. & Atkinson, C. T.) 360–374 (Wiley, 2007). https://doi.org/10.1002/9780470344668.ch20.
28. Van Woerden, H. C. et al. Differences in fungi present in induced sputum samples from asthma patients and non-atopic controls: a community based case control study. *BMC Infect. Dis.* **13**, 69 (2013).
29. Cafarchia, C. et al. Occurrence of yeasts in cloacae of migratory birds. *Mycopathologia* **161**, 229–234 (2006).
30. Talazadeh, F., Ghorbanpoor, M. & Shahriyari, A. Candidiasis in birds (Galliformes, Anseriformes, Psittaciformes, Passeriformes, and Columbiformes): a focus on antifungal susceptibility pattern of *Candida albicans* and non-albicans isolates in avian clinical specimens. *Top. Companion Anim. Med.* **46**, 100598 (2022).
31. Lagrou, K. et al. Zoonotic transmission of *Cryptococcus neoformans* from a magpie to an immunocompetent patient. *J. Intern. Med.* **257**, 385–388 (2005).
32. Nosanchuk, J. D. et al. Evidence of zoonotic transmission of *Cryptococcus neoformans* from a pet cockatoo to an immunocompromised patient. *Ann. Intern. Med.* **132**, 205 (2000).
33. Garcia-Hermoso, D. et al. DNA typing suggests pigeon droppings as a source of pathogenic *Cryptococcus neoformans* serotype D. *J. Clin. Microbiol.* **35**, 2683–2685 (1997).
34. Raso, T. F., Werther, K., Miranda, E. T. & Mendes-Giannini, M. J. S. Cryptococcosis outbreak in psittacine birds in Brazil. *Med. Mycol.* **42**, 355–362 (2004).

35. Mattsson, R., Haemig, P. D. & Olsen, B. Feral pigeons as carriers of *Cryptococcus laurentii*, *Cryptococcus uniguttulatus* and *Debaryomyces hansenii*. *Med. Mycol.* **37**, 367–369 (1999).
36. Filion, T., Kidd, S. & Aguirre, K. Isolation of *Cryptococcus laurentii* from Canada Goose guano in rural upstate New York. *Mycopathologia* **162**, 363–368 (2006).
37. Sullivan, B. L. et al. eBird: a citizen-based bird observation network in the biological sciences. *Biol. Conserv.* **142**, 2282–2292 (2009).
38. Hubálek, Z. An annotated checklist of pathogenic microorganisms associated with migratory birds. *J. Wildl. Dis.* **40**, 639–659 (2004).
39. Casadevall, A., Kontoyiannis, D. P. & Robert, V. On the emergence of *Candida auris*: climate change, azoles, swamps, and birds. *mBio* **10**, e01397–19 (2019).
40. Barrow, L. N. et al. Deeply conserved susceptibility in a multi-host, multi-parasite system. *Ecol. Lett.* **22**, 987–998 (2019).
41. Kearns, P. J., Winter, A. S., Woodhams, D. C. & Northup, D. E. The mycobiome of bats in the American Southwest is structured by geography, bat species, and behavior. *Microb. Ecol.* **86**, 1565–1574 (2023).
42. Weinstein, S. B. et al. Microbiome stability and structure is governed by host phylogeny over diet and geography in woodrats (*Neotoma* spp.). *Proc. Natl. Acad. Sci. USA* **118**, e2108787118 (2021).
43. Reese, A. T. & Dunn, R. R. Drivers of microbiome biodiversity: a review of general rules, feces, and ignorance. *mBio* **9**, e01294–18 (2018).
44. Nishida, A. H. & Ochman, H. Rates of gut microbiome divergence in mammals. *Mol. Ecol.* **27**, 1884–1897 (2018).
45. Woodhams, D. C. et al. Host-associated microbiomes are predicted by immune system complexity and climate. *Genome Biol.* **21**, 23 (2020).
46. Skeen, H. R., Cooper, N. W., Hackett, S. J., Bates, J. M. & Marra, P. P. Repeated sampling of individuals reveals impact of tropical and temperate habitats on microbiota of a migratory bird. *Mol. Ecol.* **30**, 5900–5916 (2021).
47. Skeen, H. R. et al. Intestinal microbiota of Nearctic-Neotropical migratory birds vary more over seasons and years than between host species. *Mol. Ecol.* **32**, 3290–3307 (2023).
48. Worsley, S. F. et al. Assessing the causes and consequences of gut mycobiome variation in a wild population of the Seychelles warbler. *Microbiome* **10**, 242 (2022).
49. Robinson, K., Yang, Q., Stewart, S., Whitmore, M. A. & Zhang, G. Biogeography, succession, and origin of the chicken intestinal mycobiome. *Microbiome* **10**, 55 (2022).
50. Fernandes, M. L. P. et al. Functional soil mycobiome across ecosystems. *J. Proteom.* **252**, 104428 (2022).
51. She, J.-J. et al. Defining the biogeographical map and potential bacterial translocation of microbiome in human 'surface organs'. *Nat. Commun.* **15**, 427 (2024).
52. Zhang, Z., Li, D., Xu, W., Tang, R. & Li, L. Microbiome of co-cultured fish exhibits host selection and niche differentiation at the organ scale. *Front. Microbiol.* **10**, 2576 (2019).
53. Ngunjiri, J. M. et al. Farm stage, bird age, and body site dominantly affect the quantity, taxonomic composition, and dynamics of respiratory and gut microbiota of commercial layer chickens. *Appl. Environ. Microbiol.* **85**, e03137–18 (2019).
54. Trevelline, B. K. et al. Convergent remodeling of the gut microbiome is associated with host energetic condition over long-distance migration. *Funct. Ecol.* **37**, 2840–2854 (2023).
55. Yang, Q. et al. Diversity of genotypes and pathogenicity of H9N2 avian influenza virus derived from wild bird and domestic poultry. *Front. Microbiol.* **15**, 1402235 (2024).
56. Fair, J. M. et al. Transboundary determinants of avian zoonotic infectious diseases: challenges for strengthening research capacity and connecting surveillance networks. *Front. Microbiol.* **15**, 1341842 (2024).
57. Olson, S. R. & Gray, G. C. The Trojan chicken study, Minnesota. *Emerg. Infect. Dis.* **12**, 795–799 (2006).
58. Tsiodras, S., Kelesidis, T., Kelesidis, I., Bauchinger, U. & Falagas, M. E. Human infections associated with wild birds. *J. Infect.* **56**, 83–98 (2008).
59. Thornton, M. L. Potential for long-range dispersal of aquatic phycomycetes by internal transport in birds. *Trans. Br. Mycol. Soc.* **57**, 49–59 (1971).
60. Alfonzo, A., Francesca, N., Sannino, C., Settanni, L. & Moschetti, G. Filamentous fungi transported by birds during migration across the Mediterranean Sea. *Curr. Microbiol.* **66**, 236–242 (2013).
61. Casadevall, A. & Pirofski, L. Host-pathogen interactions: Basic concepts of microbial commensalism, colonization, infection, and disease. *Infect. Immun.* **68**, 6511–6518 (2000).
62. Jones, M. R. & Witt, C. C. Migrate small, sound big: Functional constraints on body size promote tracheal elongation in cranes. *J. Evol. Biol.* **27**, 1256–1264 (2014).
63. Danesi, P. et al. Molecular diagnosis of *Emmonsia*-like fungi occurring in wild animals. *Mycopathologia* https://doi.org/10.1007/s11046-019-00353-8 (2019).
64. Rodríguez-Andrade, E. et al. A revision of *Malbranchea*-like fungi from clinical specimens in the United States of America reveals unexpected novelty. *IMA Fungus* **12**, 25 (2021).
65. Turan, D. Invasive pulmonary fungal infection caused by the fungus *Spiromastix* in an immunosuppressive patient. *Haydarpasa Numune Train. Res. Hosp. Med. J*. https://doi.org/10.14744/hnhj.2019.55823 (2019).
66. Hamm, P. S., Hutchison, M. I., Leonard, P., Melman, S. & Natvig, D. O. First analysis of human *Coccidioides* isolates from New Mexico and the Southwest four corners region: implications for the distributions of *C. posadasii* and *C. immitis* and human groups at risk. *J. Fungi* **5**, 74 (2019).
67. Jambalang, A. et al. Coccidioidomycosis in chicken pullets in Jos, Plateau State, Nigeria: a case report. *Niger Vet J*. **31**, (2010).
68. Ahasan, S. A. & Rahaman, A. Z. Mortality in Dhaka Zoo due to microbial agents. *Bangladesh J. Microbiol* **24**, 154–156 (2007).
69. World Health Organization. WHO fungal priority pathogens list to guide research, development and public health action.https://www.who.int/publications/i/item/9789240060241 (2022).
70. Gabaldón, T., Naranjo-Ortíz, M. A. & Marcet-Houben, M. Evolutionary genomics of yeast pathogens in the Saccharomycotina. *FEMS Yeast Res.* **16**, fow064 (2016).
71. Mendoza-Reyes, D. F., Gómez-Gaviria, M. & Mora-Montes, H. M. *Candida lusitaniae*: Biology, pathogenicity, virulence factors, diagnosis, and treatment. *Infect. Drug Resist.* **15**, 5121–5135 (2022).
72. Pappas, P. G. et al. Clinical practice guideline for the management of candidiasis: 2016 update by the Infectious Diseases Society of America. *Clin. Infect. Dis.* **62**, e1–e50 (2016).
73. Pfaller, M. A., Diekema, D. J., Turnidge, J. D., Castanheira, M. & Jones, R. N. Twenty years of the SENTRY antifungal surveillance program: results for *Candida* species From 1997–2016. *Open Forum Infect. Dis.* **6**, S79–S94 (2019).
74. Atasever, A. & Gümüşsoy, K. S. Pathological, clinical and mycological findings in experimental aspergillosis infections of starlings. *J. Vet. Med. Ser. A* **51**, 19–22 (2004).
75. Van Waeyenberghe, L. et al. Germination of *Aspergillus fumigatus* inside avian respiratory macrophages is associated with cytotoxicity. *Vet. Res.* **43**, 32 (2012).
76. Wernery, U. et al. Serodiagnosis of aspergillosis in falcons (*Falco* spp.) by an Afmp1p-based enzyme-linked immunosorbent assay. *Mycoses* **61**, 600–609 (2018).
77. Yamamoto, N. et al. Particle-size distributions and seasonal diversity of allergenic and pathogenic fungi in outdoor air. *ISME J.* **6**, 1801–1811 (2012).

78. Richardson, M., Bowyer, P. & Sabino, R. The human lung and *Aspergillus:* You are what you breathe in? *Med. Mycol.* **57**, S145–S154 (2019).
79. Cafarchia, C. et al. Role of birds of prey as carriers and spreaders of *Cryptococcus neoformans* and other zoonotic yeasts. *Med. Mycol.* **44**, 485–492 (2006).
80. Criseo, G., Bolignano, M. S., De Leo, F. & Staib, F. Evidence of canary droppings as an important reservoir of *Cryptococcus neoformans*. *Zentralblatt Für Bakteriol.* **282**, 244–254 (1995).
81. Li, A.-H. et al. Diversity and phylogeny of basidiomycetous yeasts from plant leaves and soil: proposal of two new orders, three new families, eight new genera and one hundred and seven new species. *Stud. Mycol.* **96**, 17–140 (2020).
82. Liu, X.-Z. et al. Towards an integrated phylogenetic classification of the *Tremellomycetes*. *Stud. Mycol.* **81**, 85–147 (2015).
83. Aboutalebian, S., Mahmoudi, S., Okhovat, A., Khodavaisy, S. & Mirhendi, H. Otomycosis due to the rare fungi *Talaromyces purpurogenus*, *Naganishia albida* and *Filobasidium magnum*. *Mycopathologia* **185**, 569–575 (2020).
84. Aghaei Gharehbolagh, S. et al. First case of superficial infection due to *Naganishia albida* (formerly *Cryptococcus albidus*) in Iran: a review of the literature. *Curr. Med. Mycol.* **3**, 33–37 (2017).
85. Bertout, S. et al. Search for *Cryptococcus neoformans/gattii* complexes and related genera (*Filobasidium*, *Holtermanniella*, *Naganishia*, *Papiliotrema*, *Solicoccozyma*, *Vishniacozyma*) spp. biotope: two years surveillance of wild avian fauna in southern France. *J. Fungi* **8**, 227 (2022).
86. Gorris, M. E., Treseder, K. K., Zender, C. S. & Randerson, J. T. Expansion of coccidioidomycosis endemic regions in the United States in response to climate change. *GeoHealth* **3**, 308–327 (2019).
87. Hijmans, R., Karney, C., Williams, E. & Vennes, C. Package 'geosphere'. https://doi.org/10.32614/CRAN.package.geosphere (2022).
88. Tobias, J. A. et al. AVONET: Morphological, ecological and geographical data for all birds. *Ecol. Lett.* **25**, 581–597 (2022).
89. Arango, A. et al. Hand-wing index as a surrogate for dispersal ability: The case of the Emberizoidea (Aves: Passeriformes) radiation. *Biol. J. Linn. Soc.* **137**, 137–144 (2022).
90. Massicotte, P., South, A. & Hufkens, K. Package 'rnaturalearth': world map data from natural Earth. https://doi.org/10.32614/CRAN.package.rnaturalearth (2023).
91. South, A., Michael, S. & Massicotte, P. Package 'rnaturalearthdata': world vector map data from natural Earth used in 'rnaturalearth'. https://doi.org/10.32614/CRAN.package.rnaturalearthdata (2024).
92. White, T. J., Bruns, T. D., Lee, S. J. & Taylor, J. W. Amplification and direct sequencing of fungal ribosomal RNA genes for phylogenetics. in *PCR protocols, a guide to methods and applications* 315–322 (Academic Press, 1990).
93. Op De Beeck, M. et al. Comparison and validation of some ITS primer pairs useful for fungal metabarcoding studies. *PLoS ONE* **9**, e97629 (2014).
94. Edgar, R. C. Search and clustering orders of magnitude faster than BLAST. *Bioinformatics* **26**, 2460–2461 (2010).
95. Edgar, R. C. *UNOISE2: improved error-correction for Illumina 16S and ITS amplicon sequencing*. http://biorxiv.org/lookup/doi/10.1101/081257 (2016).
96. Edgar, R. C. *SINTAX: a simple non-Bayesian taxonomy classifier for 16S and ITS sequences*. https://biorxiv.org/lookup/doi/10.1101/074161 (2016).
97. Abarenkov, K. et al. The UNITE database for molecular identification and taxonomic communication of fungi and other eukaryotes: Sequences, taxa and classifications reconsidered. *Nucleic Acids Res.* **52**, D791–D797 (2024).
98. Oksanen, J. et al. Community ecology package. https://doi.org/10.32614/CRAN.package.vegan (2019).
99. Nguyen, N. H. et al. FUNGuild: an open annotation tool for parsing fungal community datasets by ecological guild. *Fungal Ecol.* **20**, 241–248 (2016).
100. Lahti, L. & Shetty, S. Tools for microbiome analysis in R. https://doi.org/10.18129/B9.bioc.microbiome (2017).
101. McMurdie, P. J. & Holmes, S. phyloseq: an R package for reproducible interactive analysis and graphics of microbiome census data. *PLoS ONE* **8**, e61217 (2013).
102. Warnes, G. et al. Package 'gplots': various R programming tools for plotting data. https://doi.org/10.32614/CRAN.package.gplots (2016).
103. Paradis, E. & Schliep, K. ape 5.0: an environment for modern phylogenetics and evolutionary analyses in R. *Bioinformatics* **35**, 526–528 (2019).
104. Smith, S. Package 'phylosmith': functions to help analyze data as phyloseq objects. https://doi.org/10.5281/zenodo.3251024 (2024).
105. Mokany, K., Ware, C., Woolley, S. N. C., Ferrier, S. & Fitzpatrick, M. C. A working guide to harnessing generalized dissimilarity modeling for biodiversity analysis and conservation assessment. *Glob. Ecol. Biogeogr.* **31**, 802–821 (2022).
106. Ramsay, J. O. Monotone regression splines in action. *Stat. Sci.* **3**, 425–441 (1988).
107. Gardes, M. & Bruns, T. D. ITS primers with enhanced specificity for basidiomycetes - application to the identification of mycorrhizae and rusts. *Mol. Ecol.* **2**, 113–118 (1993).
108. Altschul, S. F. et al. Gapped BLAST and PSI-BLAST: a new generation of protein database search programs. *Nucl. Acids Res.* **25**, 3389–3402 (1997).
109. Torres-Cruz, T. J. et al. FUSARIUM-ID v.3.0: an updated, downloadable resource for *Fusarium* species identification. *Plant Dis.* **106**, 1610–1616 (2022).
110. Sayers, E. W. et al. GenBank 2024 update. *Nucleic Acids Res.* **52**, D134–D137 (2024).
111. Katoh, K. MAFFT: a novel method for rapid multiple sequence alignment based on fast Fourier transform. *Nucleic Acids Res.* **30**, 3059–3066 (2002).
112. Katoh, K. & Standley, D. M. MAFFT multiple sequence alignment software version 7: improvements in performance and usability. *Mol. Biol. Evol.* **30**, 772–780 (2013).
113. Capella-Gutiérrez, S., Silla-Martínez, J. M. & Gabaldón, T. trimAl: a tool for automated alignment trimming in large-scale phylogenetic analyses. *Bioinformatics* **25**, 1972–1973 (2009).
114. Kalyaanamoorthy, S., Minh, B. Q., Wong, T. K. F., Von Haeseler, A. & Jermiin, L. S. ModelFinder: fast model selection for accurate phylogenetic estimates. *Nat. Methods* **14**, 587–589 (2017).
115. Minh, B. Q. et al. IQ-TREE 2: new models and efficient methods for phylogenetic inference in the genomic era. *Mol. Biol. Evol.* **37**, 1530–1534 (2020).
116. Kandemir, H. et al. Phylogenetic and ecological reevaluation of the order Onygenales. *Fungal Divers.* **115**, 1–72 (2022).
117. Houbraken, J. & Samson, R. A. Phylogeny of *Penicillium* and the segregation of Trichocomaceae into three families. *Stud. Mycol.* **70**, 1–51 (2011).
118. Diezmann, S., Cox, C. J., Schönian, G., Vilgalys, R. J. & Mitchell, T. G. Phylogeny and evolution of medical species of *Candida* and related taxa: a multigenic analysis. *J. Clin. Microbiol.* **42**, 5624–5635 (2004).
119. Yu, G., Smith, D. K., Zhu, H., Guan, Y. & Lam, T. T. ggtree: an R package for visualization and annotation of phylogenetic trees with their covariates and other associated data. *Methods Ecol. Evol.* **8**, 28–36 (2017).
120. Jetz, W., Thomas, G. H., Joy, J. B., Hartmann, K. & Mooers, A. O. The global diversity of birds in space and time. *Nature* **491**, 444–448 (2012).
121. Hackett, S. J. et al. A phylogenomic study birds reveals their evolutionary history. *Science* **320**, 1763–1768 (2008).

122. Schliep, K. P. phangorn: phylogenetic analysis in R. *Bioinformatics* **27**, 592–593 (2011).
123. Jombart, T., Balloux, F. & Dray, S. *adephylo*: new tools for investigating the phylogenetic signal in biological traits. *Bioinformatics* **26**, 1907–1909 (2010).
124. Revell, L. J. phytools: an R package for phylogenetic comparative biology (and other things). *Methods Ecol. Evol.* **3**, 217–223 (2012).
125. Thompson, C. W. et al. Preserve a voucher specimen! The critical need for integrating natural history collections in infectious disease studies. *mBio* **12**, e02698–e02720 (2021).
126. Colella, J. P. et al. Leveraging natural history biorepositories as a global, decentralized, pathogen surveillance network. *PLOS Pathog.* **17**, e1009583 (2021).
127. Salazar-Hamm, P. S. et al. Data files – Phylogenetic and ecological drivers of the avian lung mycobiome and its potentially pathogenic component. [Data set]. *Zenodo* https://zenodo.org/records/15098514 (2025).

Acknowledgements

This project was made possible utilizing the frozen collections preserved at the Genomic Resources Division in the Museum of Southwestern Biology at the University of New Mexico (UNM) and the support of New Mexico Department of Game and Fish personnel from the Bernardo hunter check station. We thank Matthew Baumann, Selina Bauernfeind, Trinity Casaus, Marialejandra Castro Farías, Sarah Shrum Davis, Cory Griego, Tina Guo, Alesia Hallmark, Paige Handley, Andy Johnson, Ryan Laughlin, Ethan Linck, Diana Macias, Xena Mapel, Aaron Matins, Kristen Oliver, David Tan, and Brenda Villanueva for assistance with sample collection, specimen preparation, and curation. We additionally would like to thank the UNM Department of Biology's Molecular Biology Facility, supported by the UNM Center for Evolutionary & Theoretical Immunology (CETI) under National Institutes of Health grant P30GM110907, and the UNM Center for Advanced Research Computing (CARC) for analytical support. Additional funding was acquired through student research awards from the New Mexico Ornithological Society (MAM), the American Ornithological Society (CRG), and the UNM Graduate and Professional Student Association (PSS-H). This work was also partially supported by a National Science Foundation PIPP Phase I grant (NSF 2155222, Joseph Cook PI), the UNM Sevilleta Field Station Endowment fund, and the UNM Museum of Southwestern Biology.

Author contributions

Conceptualization: P.S.S.-H., C.R.G., C.C.W., and D.O.N.; investigation: P.S.S.-H., C.R.G., M.S., E.F.G., S.S.B., J.L.W., O.M.T., K.N.M., M.B., C.C.W., and D.O.N.; formal analysis: P.S.S.-H., C.R.G., and M.A.M.; data curation: P.S.S.-H. and C.R.G.; supervision: C.C.W. and D.O.N.; writing—original draft preparation: P.S.S.-H. and C.R.G.; writing—review and editing, M.A.M., M.S., K.N.M., M.B., C.C.W., E.F.G., S.S.B., O.M.T., J.L.W., and D.O.N.; funding acquisition: P.S.S.-H., C.R.G., M.A.M., C.C.W., and D.O.N. All authors have read and agreed to the published version of the manuscript.

Competing interests

The authors declare no competing interests.

Ethics

All bird tissues were collected from salvaged and legally hunted birds donated to the Museum of Southwestern Biology under state (NMDGF 3217) and federal (USFWS MB094297) scientific salvage permits. No live birds were euthanized or harmed for this study.

Additional information

Supplementary information The online version contains supplementary material available at https://doi.org/10.1038/s42003-025-08041-8.

Correspondence and requests for materials should be addressed to Paris S. Salazar-Hamm or Chauncey R. Gadek.

Peer review information *Communications Biology* thanks the anonymous reviewers for their contribution to the peer review of this work. Primary handling editors: Madhava Meegaskumbura and Joao Valente. A peer review file is available.